SUPPORTING ONLINE MATERIAL

MATERIALS AND METHODS

Experimental animals

Captive-born hatchling Burmese pythons were purchased commercially (Strictly Reptiles, Hollywood, FL, USA) and housed individually at 28–32°C under a 14h/10h light/dark cycle. Pythons were fed rats as meals bi-weekly and had continuous access to water. Rats were obtained from the rodent facility at the University of Colorado at Boulder and kept frozen; rats were thawed in clean warm water before feeding. Python care and study were conducted under approval from the IACUC of the University of Colorado and the University of Alabama. Prior to experimentation, pythons were fasted for a minimum of 30 days to ensure that they were post-absorptive. Pythons used in this study were of both sexes, between 6 and 12 months old, and weighed approximately 400 g. To induce the postprandial response, pythons were fed rodent meals equivalent to 25% of their body mass. Prior to dissection and tissue collection, pythons were sedated with Isofluorane and subsequently euthanized. Tissue to be used for non-histochemical analyses and plasma were collected from four pythons at each prandial state (0, 0.5, 1, 2, 3, 6 and 10 DPF) Samples were snap-frozen in liquid nitrogen and stored at -80°C prior to experimentation. For the bromodeoxyuridine (BrdU) incorporation assay, two pythons were fasted for 30 days followed by four intraperitoneal injections per python with BrdU (100 mg/kg every two hours) upon feeding.

Histological Analyses

Python or mouse ventricle was either fixed in 10% neutral-formalin buffer or snap frozen in liquid nitrogen. H&E and Masson's Trichrome staining was performed using standard procedures. For BrdU staining, sections were pretreated in 2N HCl to quench endogenous peroxidase activity, treated with 3.0% hydrogen peroxide, and further retrieved with Proteinase K (S3020; Dako, Carpinteria, CA, USA). The rat anti-mouse BrdU antibody (Mas 250b; Harlan Sera Laboratories, Loughborough, UK) was prepared at a working dilution of 5 mg/ml. As a positive control, python intestinal sections were also stained as previously described (*27*).

For mitochondria staining, a 3.0% hydrogen peroxide solution was used to quench endogenous peroxidase activity. The mouse anti-human MTCO2 (COX2) antibody (NB600-556; Novus Biologicals, Littleton, CO, USA) was prepared at a 2 µg/ml working dilution. For NADH-tetrazolium reductase (NADH-TR) staining, snap-frozen ventricles were cryo-embedded, sectioned at 20 µm, and stained as described previously (*28*). For neutral lipid staining, mouse or python ventricle was fixed in 10% neutral-formalin buffer or snap frozen, stained with Oil red O, and counterstained with hematoxylin. As a positive control, mouse aortic sections from an induced-heart disease model were also stained.

For quantification of mouse cardiomyocyte cross-sectional area, left ventricle was snap frozen, sectioned at 20 µm, incubated with Texas Red-conjugated wheat germ agglutinin (WGA; W21405, Invitrogen/Molecular Probes,

Carlsbad, CA, USA) at 10 μg/mL for 30 min, rinsed 3x in PBS, and mounted using ProLong® Gold antifade reagent with DAPI (Invitrogen). Mean cardiomyocyte cross-sectional area was determined on at least 2 representative fields of view from n=6 animals per group (BSA or FA infused).

Western blotting

Mouse or python ventricle was homogenized in RIPA buffer (50mM Tris-HCl pH 8, 150mM NaCl, 0.5% Sodium Deoxycholate, 1% NP-40, 0.1% SDS), supplemented with protease inhibitors (Complete EDTA free; Roche, Indianapolis, IN, USA; 1mM PMSF) and phosphatase inhibitors (Cocktail Set I, Calbiochem/EMD, Gibbstown, NJ, USA; 1mM Sodium Orthovanadate; 20mM Sodium Fluoride), centrifuged at 14,000 *g* for 5 minutes. 15 µg (mouse) or 25 µg (python) of protein from the supernatant was resolved by SDS-PAGE and analyzed by Western blot using antibodies from Cell Signaling (Danvers, MA, USA), unless indicated: p-p70S6K (Thr421/Ser424, #9204), total p70S6K (#9202), p-AMPK (Thr172, #2535), total AMPK (#2793), p-Akt (Ser473, #4058), total Akt (#9272), p-GSK3β (Ser9, sc-11757; Santa Cruz, Paso Robles, CA, USA), total GSK3β (sc-7291, Santa Cruz), p-mTOR (Ser2448, #2971) and total mTOR (#2983).

Cell Culture and Adenoviral Infection

Neonatal rat ventricular myocytes (NRVMs) were prepared according to the method described in Waspe et al. (*29*). In brief, cells were obtained from the

hearts of Sprague–Dawley rat pups (1-2 days old), isolated by trypsinization, and plated in Minimum Essential Medium (MEM, 11575; Gibco/Invitrogen, Carlsbad, CA, USA) with 10% calf serum. After 24 hours in culture, cells were transferred to serum-free medium supplemented with transferrin and insulin (10 ug/ml each). Cells were maintained in 60- or 35-mm gelatinized culture dishes at a density of 100,000 cells/ml. To assay NFAT activity, cells were transduced with an adenoviral NFAT reporter construct (kindly donated by Dr. Molkentin) at a multiplicity of infection of 20 plaque-forming units/cell.

Plasma extraction, NRVM Treatment, Cell Size Quantification and Immunostaining.

Blood samples were obtained from euthanized pythons in blood collection tubes with 7.5% K_3 EDTA solution (Vacutainer®, BD, Franklin Lakes, NJ, USA). The collected blood samples were centrifuged at 3000 x *g* for 10 min. to separate plasma, then aliquoted and snap-frozen in liquid nitrogen. For longer storage, plasma samples were kept at -80°C. Plasma used for NRVM treatments was heat inactivated at 58°C for 30 min. NRVMs were supplemented with heat-inactivated plasma at final concentration of 2% (unless stated otherwise) for 48 hours. Immunofluorescence was performed according to Harrison et al. (*4*) using α-actinin antibody (A5044, Sigma-Aldrich, St. Louis, MO, USA) and Alexa Fluor 488 anti mouse antibody (A21202, Invitrogen/Molecular Probes, Carlsbad, CA, USA). Images were captured at a 40x magnification with a fluorescence microscope (Nikon E800) equipped with a digital camera (AxioCam). Cell size

was determined using the Coulter Counter Multisizer 3 (Beckman Coulter, Brea, CA, USA). Briefly, cells were trypsinized, resuspended in PBS supplemented with 5% calf serum and 1 mM EDTA, and kept on ice until analyzed.

Synthesis of SSO and Inhibition of Fatty Acid Transport

Unlabeled sulfo-succinimidyl oleate (SSO) was synthesized as described by Harmon *et al.* (*30*) by the Sammakia Laboratory (University of Colorado, Department of Chemistry). CD36 inhibition studies were performed by treating NRVMs with 400 μM SSO dissolved in DMSO (1% final concentration) for 30 min. After the treatment, NRVMs were washed twice with serum free media to remove SSO/DMSO before adding the python plasmas. A vehicle control of DMSO (final concentration 0.1%) was added to NRVMs that were not supplemented with SSO.

Quantitative real-time PCR (qPCR)

Total RNA was extracted from mouse or python ventricle and NRVMs using TRI Reagent (Invitrogen). 0.5 to 2.0 μg of RNA was reverse transcribed into cDNA using the SuperScript III first-strand cDNA synthesis kit (Invitrogen). Quantitative real time PCR reactions were performed using the ABI7300 system (Applied Biosystems, Foster City, CA, USA) and the Power SYBR Green PCR Master Mix (Applied Biosystems). Primer sequences are available in the supplemental documents (Tables S1-S3). Python gene-specific primers were generated from our laboratory's sequencing of the python heart transcriptome

using the Illumina platform (*13*). Gene expression was normalized to either 18S ribosomal RNA (mouse) or hypoxanthine guanine phosphoribosyl transferase (HPRT, python) and depicted as normalized mRNA expression.

Mn-Superoxide Dismutase and Caspase Activity

Myocardial Mn-superoxide dismutase (Mn-SOD) activity was measured using a Cu/Zn, Mn-, and Fe-SOD activity kit (Cayman Chemical, Ann Arbor, MI, USA). For the assay, python ventricle was homogenized in 20 mM HEPES buffer (pH 7.2) containing 1 mM EGTA, 210 mM mannitol, and 70 mM sucrose per gram of tissue. Homogenates were then centrifuged at 1500 ×g for 5 min. at 4°C and the resulting supernatant further centrifuged at 10,000 ×g for 15 min at 4°C. The pellet (containing mitochondrial Mn-SOD) was resuspended in 20 mM HEPES buffer with 1 mM potassium cyanide added to inhibit Cu/Zn-SOD and extracellular SOD activity (*31*). SOD activity is expressed as U/ml*mg protein.

NRVM caspase activity was measured as described previously (*6*). Briefly, Caspase-3 activity was determined by monitoring the rate of cleavage of a fluorogenic caspase-3 specific substrate (Acetyl-AspGluValAsp-AMC; Calbiochem/Merck, Rockland, MA, USA). NRVMs were mechanically disrupted in an ice-cold lysis buffer containing: (in mmol/L) Tris(hydroxymethyl)-aminomethane (20); NaCl (137); EDTA (0.2); EGTA (0.5); Triton X-100 (1%); Glycerol (10%) (pH 7.4). Cleavage of the substrate was monitored by excitation at 380 nm and emission at 460 nm with a Fluorskan Ascent Microplate Fluorometer (Thermo Electron Corp., Milford, MA, USA). Caspase-3 activity was

determined by calculating the slope of the linear portion of the cleaved substrate and then normalized to protein content (fluorescent units/minute/mg protein). Activity was normalized to the activity of the serum free (NP) control.

Triglyceride and Free-Fatty Acid Analysis

Plasma triglyceride (TAG) and non-esterified free-fatty acid (NEFA) content were measured using kits from Wako Diagnostics (L-type TG H and NEFA-HR 2) per the manufacturer's instructions (Wako Diagnostics, Richmond, VA, USA). Ventricular TAG and NEFA composition of was determined using thin-layer chromatography (TLC). For TLC, total lipids were extracted from ventricles using a modified Folch extraction (*32*) using chloroform-methanol-formic acid (10:10:1 v/v). 25 µL of the organic phase containing the lipids from each sample was spotted onto silica gel G TLC plates (Z12,277-7, Sigma-Aldrich) and run using a hexane:diethyl ether:acetic acid (40:10:1) mobile phase and developed using iodine. For gas chromatography (GC) analysis, total lipids extracted from plasma as previously described were transesterified in 1% sulfuric acid in methanol 85 ^{o}C for 1 hour. The resulting fatty acid methyl esters were extracted from the mixture with hexane. Fatty acid methyl esters were separated and quantified by capillary gas chromatography (Model 6890N, Agilent Technologies, Santa Clara, CA, USA) equipped with a DB-23 column (30m x 250µm x 0.25µm) and a flame-ionization detector.

Preparation of Fatty Acid-BSA Complexes

Palmitic (C16:0), palmitoleic (C16: I), myristic (C14:0), oleic (C18:1), linoleic (C18:2), and arachidonic (C20:4) acids (Sigma-Aldrich) were complexed with fatty acid-free bovine serum albumin (BSA, A6003, Sigma-Aldrich) according to the method described by de Vries et al (*22*). BSA and FFA/BSA were dissolved in NRVM culture media (glucose-free MEM with PB12 and HEPES) or sterile saline (0.9%) to yield a final BSA concentration of 10%, sterile filtered, aliquoted, and stored at -20°C. The actual concentration of FA in the media or saline was measured as previously described and averaged 7 mM. Accordingly, the FFA/BSA ratio in the medium amounted to *3.3* to 1.

In Vivo Infusions in Pythons and Mice

Boluses (0.5 mL) of python plasma (fasted or fed [2 DPF]), bovine seum albumin (BSA; 10% in physiological saline), or the mixture of palmitoleic (C16:1), myristic (C14:0), and palmitic (C16:0) acids in the molar ratio of 1:6:16 (FA stock solutions were ~7mM) were infused through surgically implanted catheters at 12-hr intervals into the hepatic vein of pythons over a 48-hr period (4 infusions per snake). Plasma originated from snakes that were siblings to those infused. Catheters (PE 90) were implanted under isoflurane anesthesia cranial to the liver and exteriorized through an opening in the body wall. Snakes typically recovered from anesthesia within 30 min and were then maintained at a constant 30°C until dissection and tissue collection.

ALZET® mini-osmotic pumps (Model 2001, Durect Corporation, Cupertino, CA, USA) containing either BSA (10% in sterile saline), the mixture of

C16:0, C14:0, and C16:1 described above, or a control mixture of C20:4, C18:1, and C18:2 in the 1 DPF molar ratio (1:27:40) were implanted subcutaneously in mice under inhaled isoflurane anesthesia. Pumps delivered 1 μL per hour for 7 days; mice were sacrificed on the 7th day after implantation.

Statistics

Data depicted as mean ± SE unless otherwise noted. Data were analyzed using Statview™ 5.0 statistical software (SAS Institute, Cary, NC, USA). Statistical comparisons were performed using ANOVA combined with the Fisher's paired least significant difference post hoc test. Statistical significance was set at $p<0.05$.

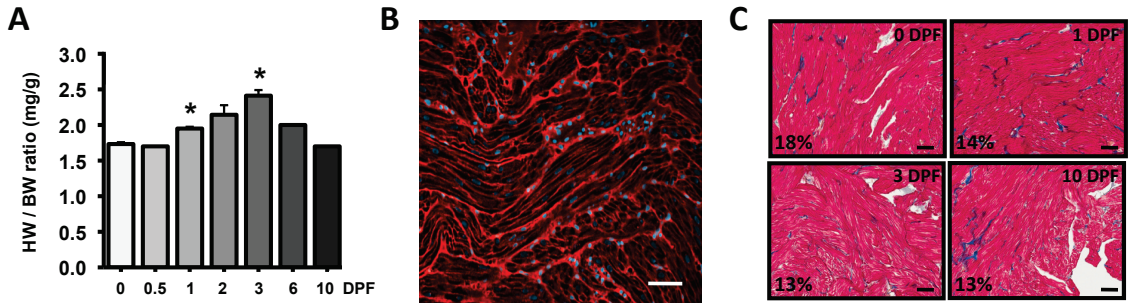

Figure S1: Postprandial cardiac hypertrophy in the absence of alterations in collagen deposition. (**A**) Python heart weight to body weight ratios (HW/BW) determined at different time points after feeding showing progression and regression of cardiac growth; cardiac growth profile is similar to the effect obtained *in vitro* in NRVMs treated with python plasma (see Figure 3A). Error bars represent ±SE; n=4 per time point; *$p<0.05$ versus 0 DPF. (**B**) Wheat germ agglutinin staining of python ventricle reveals complex pattern of cellular orientations. Scale bar = 50 μm. (**C**) The percent collagen content of the python heart (~13-18%) is higher than typically seen in the rodent heart (~1-2%) and relatively unchanged during the postprandial period. Representative fields of Masson trichrome-stained heart sections showing calculated percent collagen content (blue). Scale bar = 50 μm.

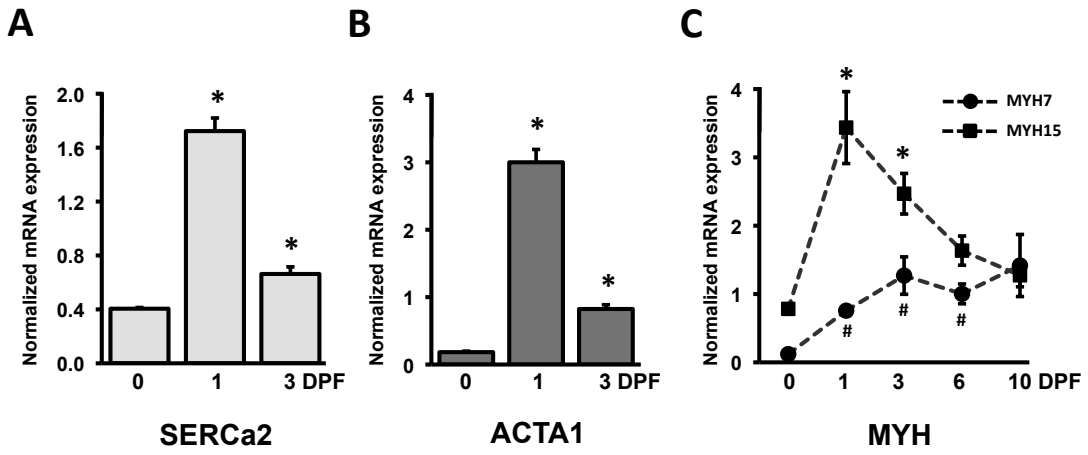

Figure S2: Alterations in gene expression in the postprandial python heart. **(A)** SERCa2 and **(B)** α-skeletal actin (ACTA1) mRNA levels were significantly increased at 1 and 3 days post-fed (DPF); **(C)** mRNA levels of both MYH15 (black squares) and MYH7 (black circles) were elevated post-feeding. Error bars represent ±SE; n=4 per time point; *$p<0.05$ versus 0 DPF; #$p<0.1$ versus 0 DPF.

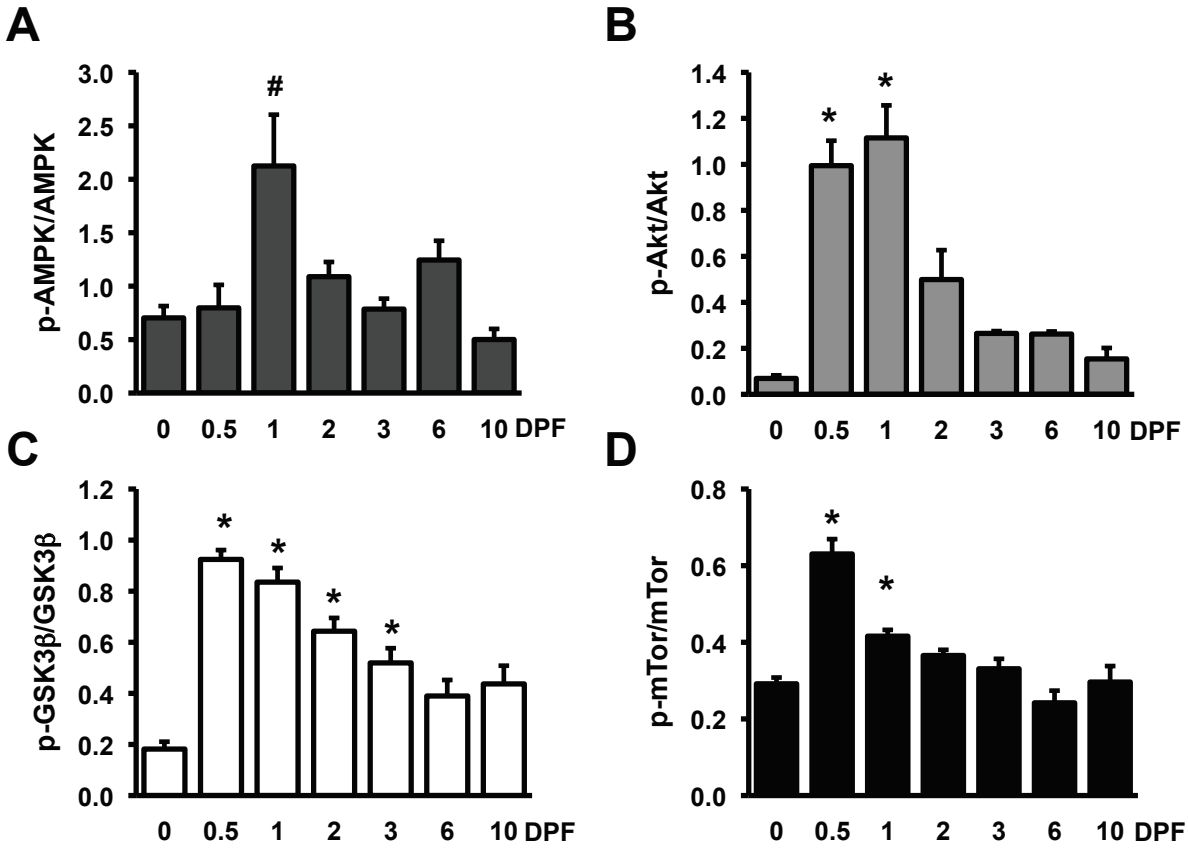

Figure S3: Activation of signaling pathways associated with protein synthesis in python heart throughout digestion. (**A**) The ratio of p-AMPK/AMPK was significantly increased at 1 DPF. (**B**) The ratio of p-Akt/Akt was significantly increased at 0.5 and 1 DPF. (**C**) The ratio of p-GSK3β/GSK3β was significantly increased at 0.5, 1, 2, and 3 DPF. (**D**) The ratio of p-mTor/mTor was significantly increased at 0.5 and 1 DPF. Error bars represent ±SE; n=4 per time point; *$p<0.05$ versus 0 DPF; #$p<0.1$ versus 0 DPF.

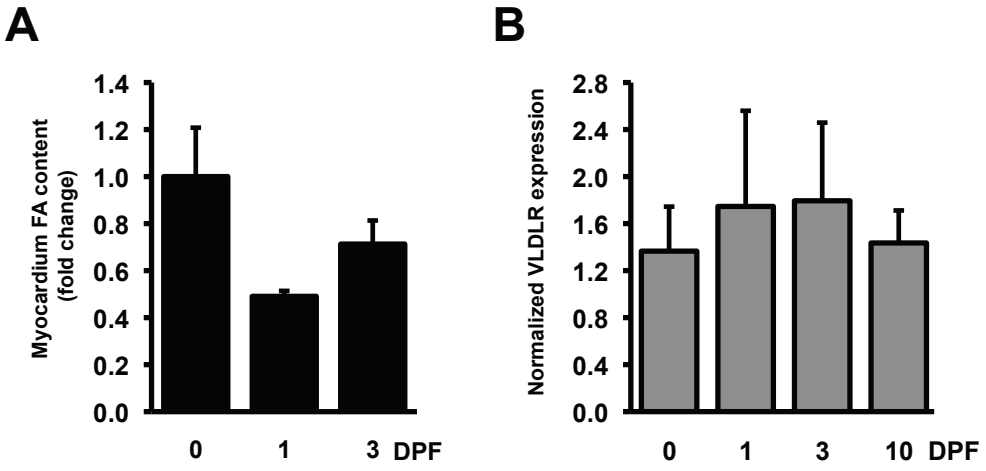

Figure S4: Elevated plasma fatty acid and triglyceride levels do not induce lipid accumulation in python myocardium. (**A**) The postprandial ventricular myocardium does not show an increase in non-esterified free fatty acid (FA) content at 1 or 3 days after feeding. Fatty acids were extracted from heart tissue and analyzed by TLC. (**B**) mRNA transcript levels of VLDLR are not changed in hypertrophied heart.

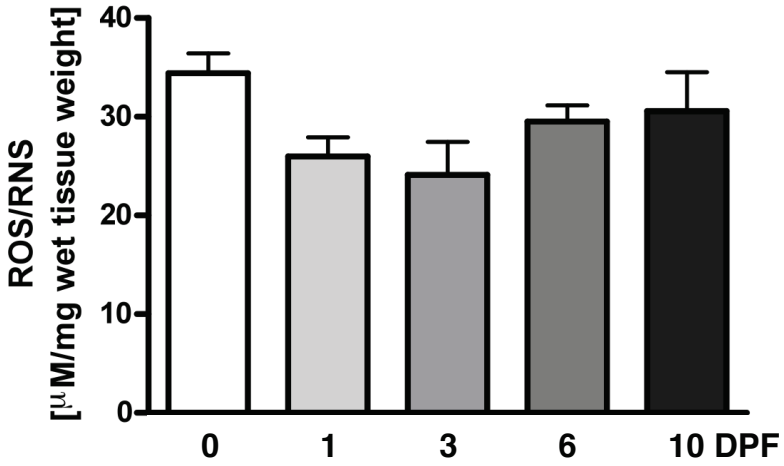

Figure S5: Ventricular reactive oxygen/nitrogen species content is unchanged during digestion in the postprandial python. Reactive oxygen/ nitrogen species (ROS/RNS) content was determined using a fluorometric assay. Error bars represent ±SE; n=2 per time point.

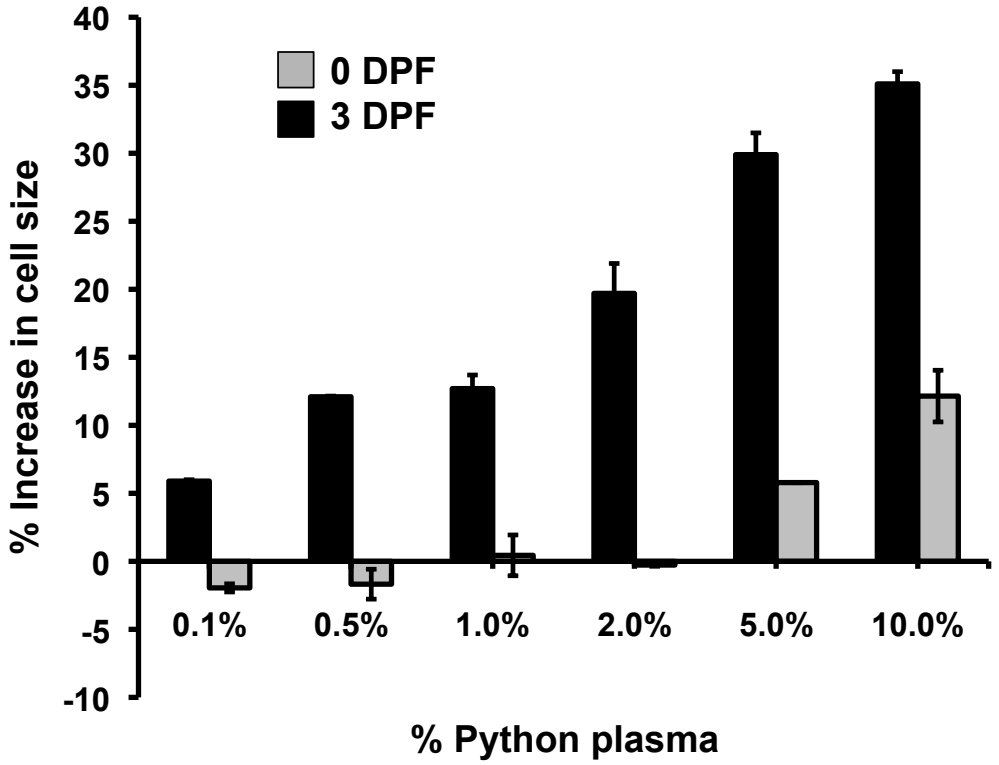

Figure S6: Fed python plasma induces dose-dependent cellular hypertrophy in neonatal rat ventricular myocytes. Cell size was measured 48 hours after culturing NRVMs in the presence of plasma from either 0 or 3 DPF pythons at concentrations ranging from 0.1% to 10.0%. Error bars represent ±SE; n=3 per condition.

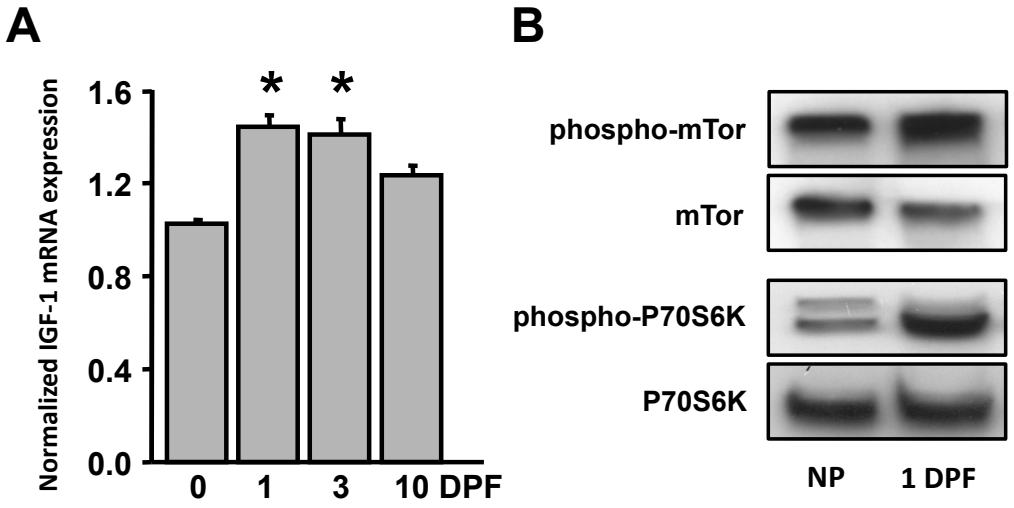

Figure S7: Fed python plasma induces IGF-1 mRNA and activates signaling pathways associated with protein synthesis in neonatal rat ventricular myocytes. (**A**) IGF-1 mRNA was significantly increased by 1 and 3 DPF plasma as compared to 0 DPF plasma. (**B**) Fed (1 DPF) plasma treatment stimulated phosphorylation of p70S6K and mTOR. Error bars represent ±SE; n=2 per condition; *$p<0.05$ versus 0 DPF.

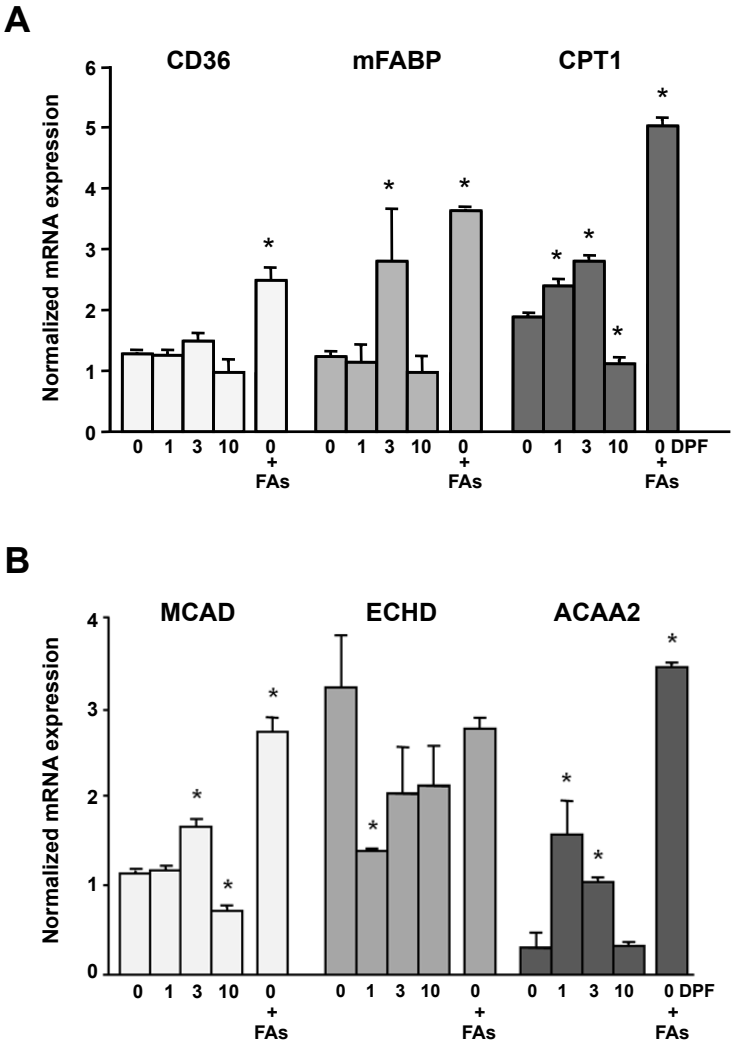

Figure S8: Treatment of neonatal rat ventricular myocytes with python plasma or fatty acids alters the mRNA levels of genes associated with fatty acid transport, handling and oxidation. (**A**) FABP3 mRNA expression was increased in NRVMs treated with 3 DPF plasma; CPT1 mRNA expression was increased in NRVMs treated with 1 and 3 DPF plasma and reduced in NRVMs treated with 10 DPF plasma. The mRNA expression of CD36, FABP3, and CPT1 was increased in NRVMs treated with fasted plasma plus the combination of C14, C16, and C16:1 (0 DPF + FAs). (**B**) MCAD mRNA expression was increased in NRVMs treated with 3 DPF plasma and reduced in NRVMs treated with 10 DPF plasma. ECHD mRNA expression was reduced in NRVMs treated with 1 DPF plasma. ACAA2 mRNA expression was increased in NRVMs treated with 1 and 3 DPF plasma. The mRNA expression of MCAD and ACAA2 was increased in NRVMs treated with fasted plasma plus the combination of C14, C16, and C16:1 (0 DPF + FAs). Error bars represent ±SE; n=4 per condition; *$p<0.05$ versus 0 DPF plasma.

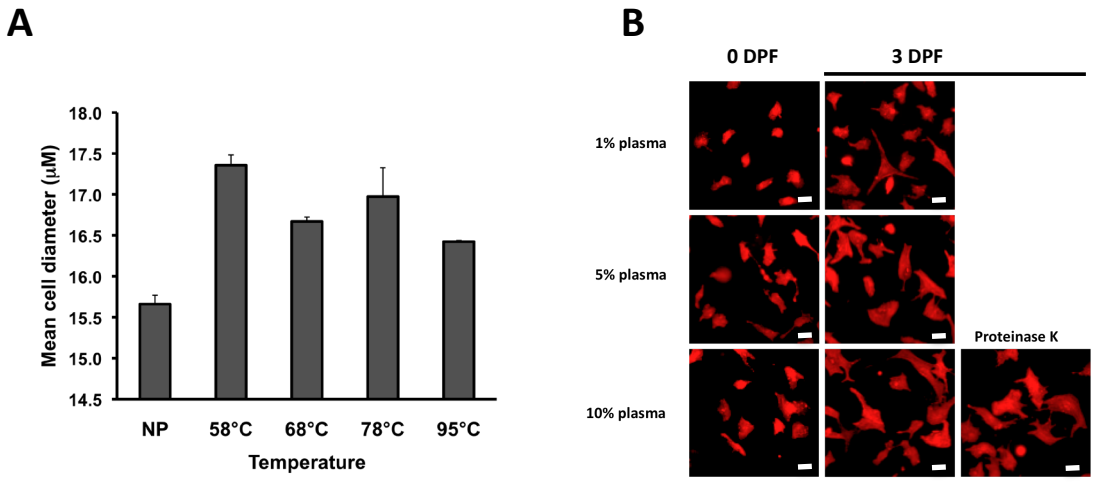

Figure S9: The hypertrophic effects of python plasma are resistant to heat inactivation and Proteinase K treatment. (**A**) Heat inactivation ranging from 58°C to 95°C had minimal effects on the hypertrophic effects of 3 DPF python plasma in neonatal rat ventricular myocytes (NRVMs). (**B**) Proteinase K digestion did not block the pro-hypertrophic effects of fed (3 DPF) python plasma in NRVMs. NRVMs were immunostained for a-actinin to reveal cell size and sarcomere organization. Error bars represent ±SE; n=3 per condition. Scale bar = 20 μm.

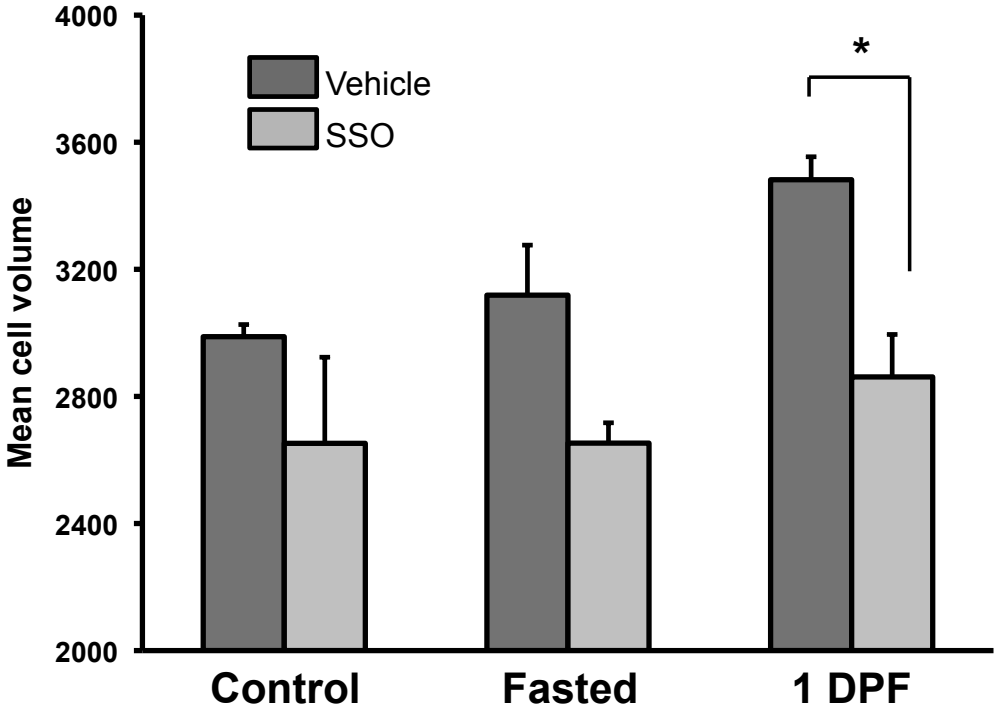

Figure S10: Inhibition of fatty acid transport blocks python plasma-induced neonatal rat ventricular myocyte hypertrophy. NRVMs were treated with either no plasma (Control), 0 DPF, or 1 DPF python plasma in absence or presence of the CD36 inhibitor sulfosuccinimidly-oleate (SSO). NRVM hypertrophy due to fed plasma was significantly reduced by SSO treatment. Error bars represent ±SE; n=3 per condition; *$p<0.05$ versus vehicle.

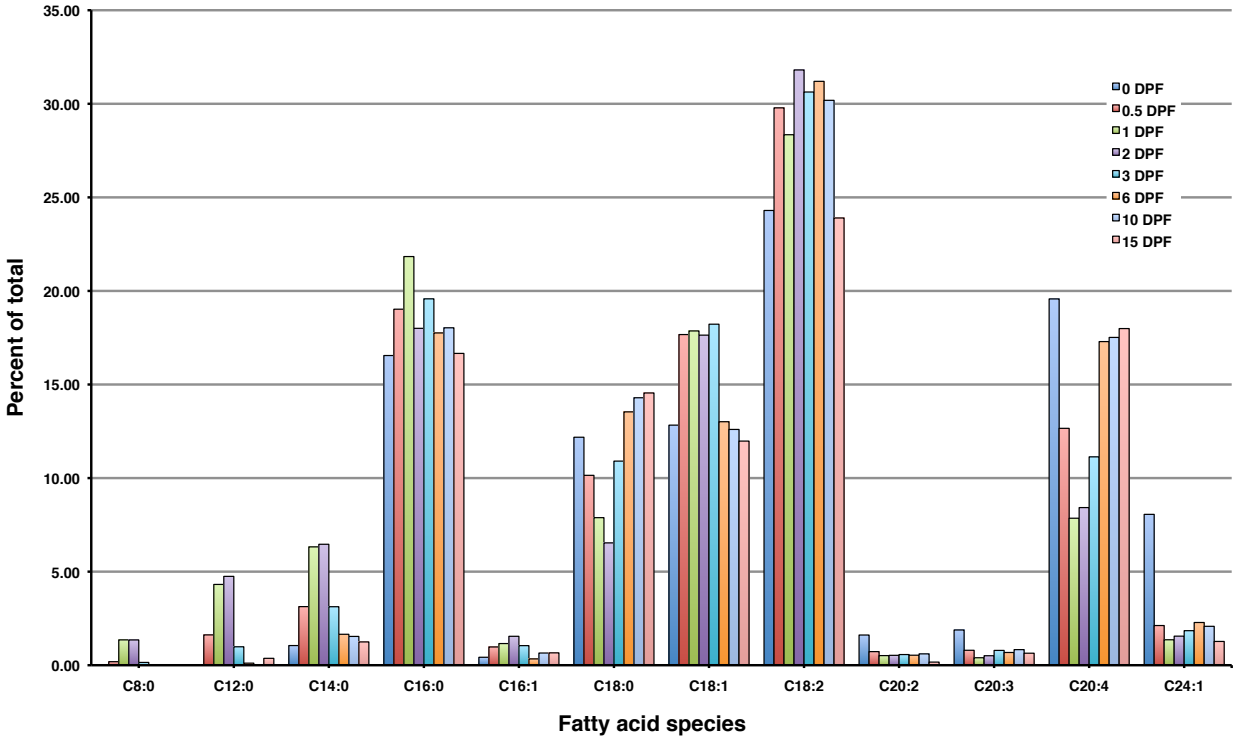

Figure S11: Gas chromatography on python plasma reveals a complex pattern of change in circulating lipid species during the postprandial time period. Fatty acid class composition analysis in python plasma at different time points after feeding by gas chromatography. The concentration of the individual FAs was expressed as the percentage of total FA concentration at each time point.

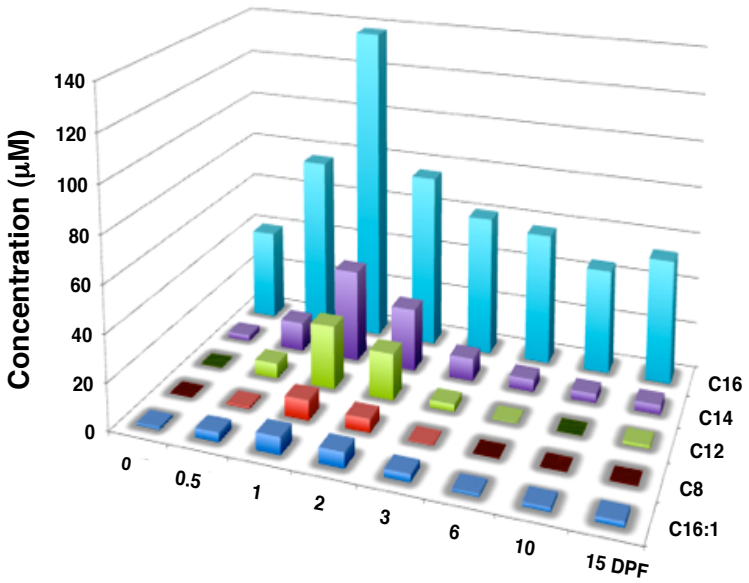

Figure S12: Plasma concentration of candidate fatty acids. Concentrations (μM) of (caprylic [C8:0], lauric [C12:0], myristic (C14:0), palmitic [C16:0], and palmitoleic [C16:1n7] acid) as determined by gas chromatography (FAs presented in order of increasing 0 DPF concentration).

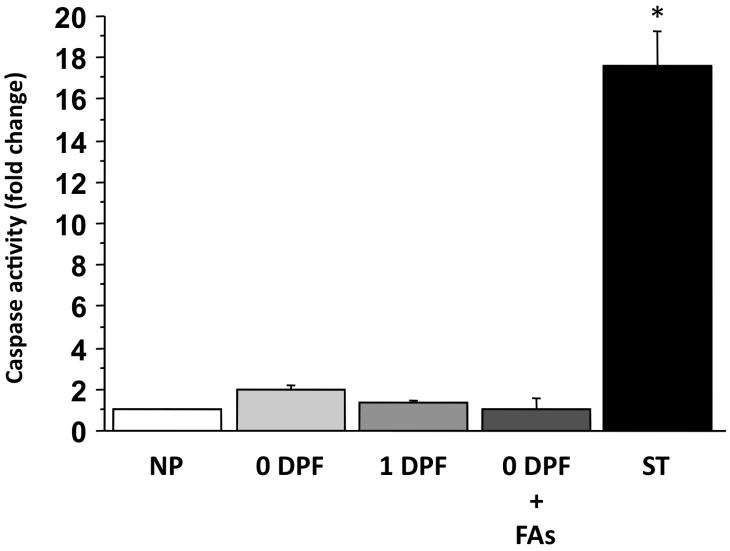

Figure S13. Treatment of neonatal rat ventricular myocytes with python plasma or fasted plasma plus fatty acids does not trigger apoptosis. Treatment of NRVMs with no plasma (NP), 0 DPF, 1 DPF, or fasted plasma plus C14:0, C16:0, and C16:1n7 (0 DPF + FAs) for 24 hours had no effect on caspase activity. Staurosporine (ST; 10 mM) was used a positive control. Error bars represent ±SE; n=3 per condition; *$p<0.05$ versus no plasma (NP).

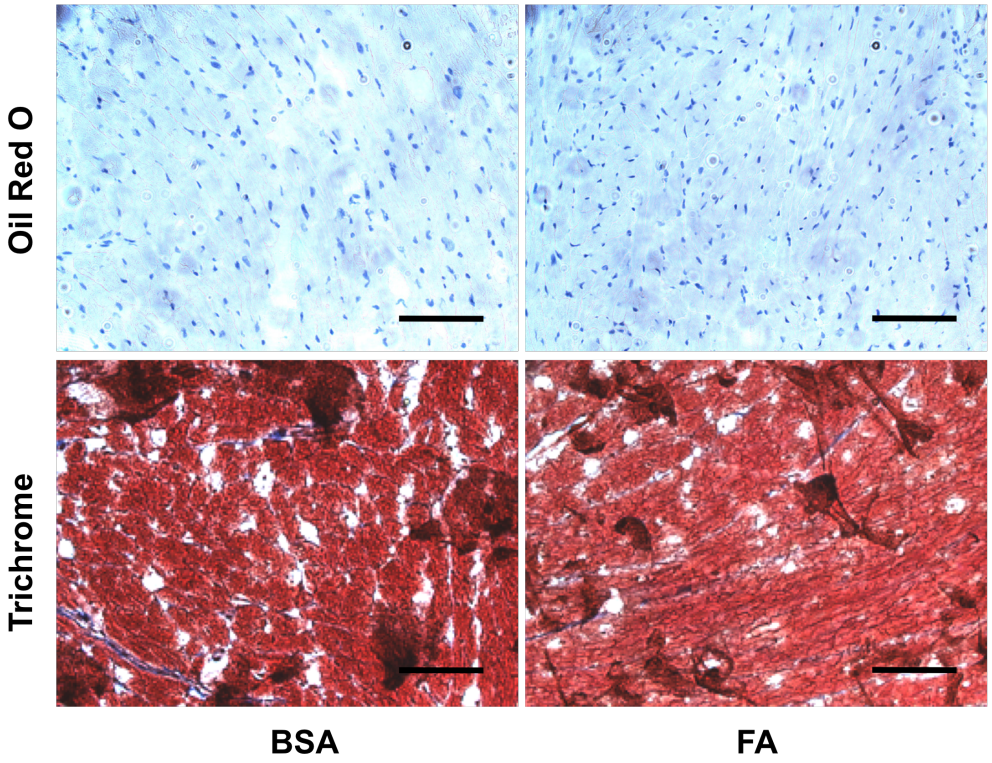

Figure S14: Fatty acid infusion in mice does not alter cardiac lipid deposition or fibrosis. There was no evidence of cardiac lipid accumulation (Oil Red O staining) or alterations in cardiac fibrosis (Mason Trichrome staining) following 7 days of fatty acid (C14:0, C16:0, and C16:1) infusion. Scale bar = 50 μm.

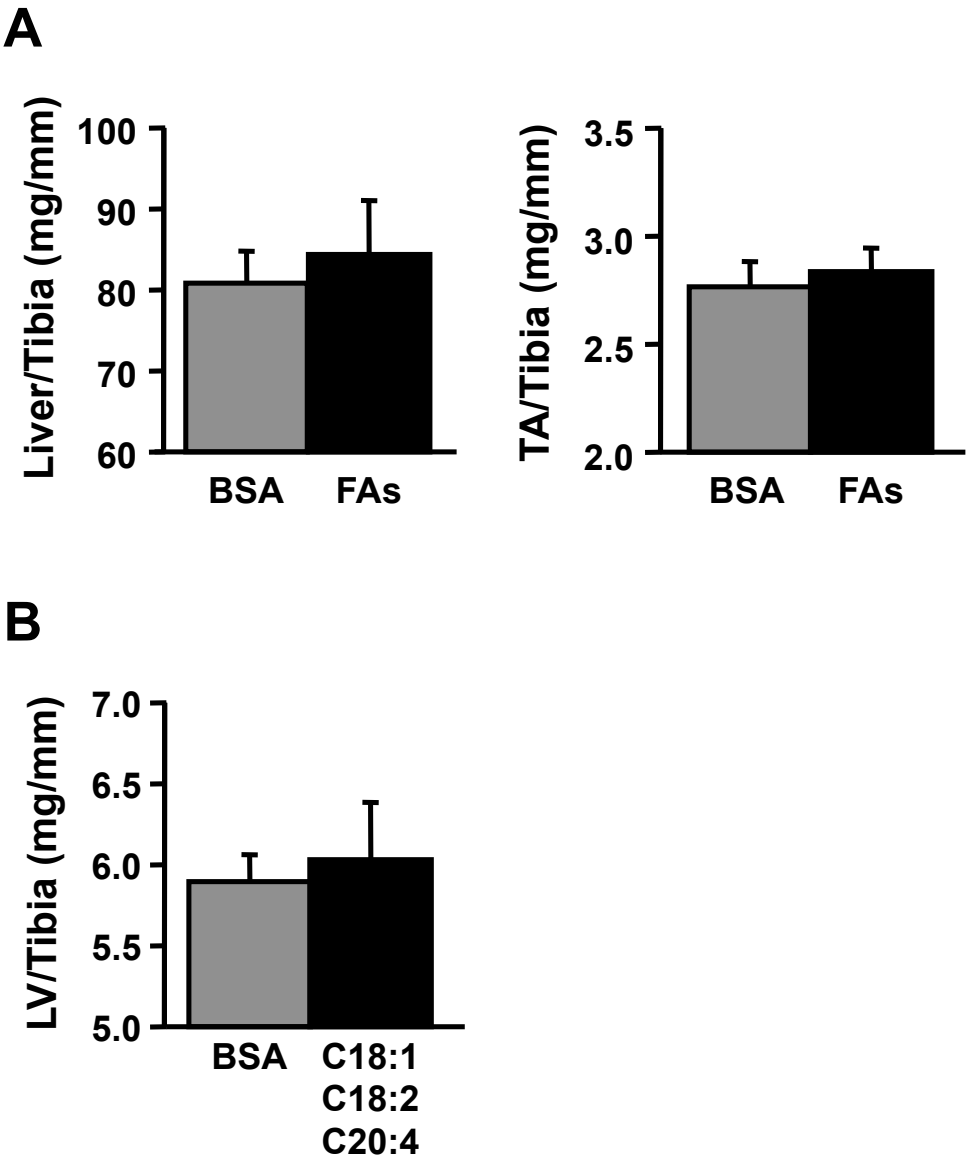

Figure S15: Fatty acid-induced hypertrophy is cardiac- and lipid composition-specific. (**A**) Infusion of C14:0, C16:0, and C16:1 (FAs) over a 7 day period had no effect on the mass of the liver or the tibialis anterior (TA). Tibia length (mm) was used to normalize for body size. (**B**) Infusion of a control mixture of C18:1, C18:2, and C20:4 over a 7 day period had no effect on left ventricular mass. Error bars represent ±SE; n=3 (**B**) or 6 (**A**) per condition.

Table S1: Primer Sequences for Mouse Genes (5' – 3')

ACTA1 F	**ATGAGCGTTTCCGTTGCCC**
ACTA1 R	**CCCTGACATGACGTTGTTG**
ANF F	AGGAGAAGATGCCGGTAGAAGA
ANF R	GCTTCCTCAGTCTGCTCACTCA
MYH6 F	**ACATTCTTCAGGATTCTCTG**
MYH6 R	**CTCCTTGTCATCAGGCAC**
MYH7 F	TTCCTTACTTGCTACCCTC
MYH7 R	CTTCTCAGACTTCCGCAG

Table S2: Primer Sequences for Rat Genes (5' – 3')

ACAA2 F	**CCTGGCTGCAAAATACAACA**
ACAA2 R	**CATGGTCTGTTTGCCCTTCT**
ACTA1 F	CCACCTACAACAGCATCATGAAGT
ACTA1 R	GACATGACGTTGTTGGCGTACA
ANF F	**GCGAAGGTCAAGCTGCTT**
ANF R	**CTGGGCTCCAATCCTGTCAAT**
CD36 F	ACAGTTTGCAAAACGACTGC
CD36 R	CGATGGTCCCAGTCTCATTT
CPT1 F	**TCTCAGCCTCTACGGCAAAT**
CPT1 R	**TGCCCATGAGTGTTCTGTGT**
ECHD F	TGGCGATATGCTCTGTGAAG
ECHD R	AGGGATCAGGTTTGTGGATG
IGF1 F	**CTGAGCTGGTGGACGCTCTTC**
IGF1 R	**CACTCATCCACAATGCCCGTCT**
MCAD F	GGAGCAGGTTTCAAGATTGC
MCAD R	GTTTTCCTGTCCAGGGCATA
mFABP F	**CCCGTGTAAGCGTAGTCTCC**
mFABP R	**GGTCACAGCAGATGACAGGA**
MYH6 F	CCTGTCCAGCAGAAAGAGC
MYH6 R	CAGGCAAAGTCAAGCATTCATATTTATTGTG
MYH7 F	**CGCTCAGTCATGGCGGAT**
MYH7 R	**GCCCCAAATGCAGCCAT**
SERCa2 F	GGCCAGATCGCGCTACA
SERCa2 R	GGGCCAATTAGAGAGCAGGTTT

Table S3: Primer Sequences for Python Genes (5' – 3')

ACAA2 F	**GAAGTTGGCAGTTGGAGGAG**
ACAA2 R	**AATCTCTGCGAGGTCTGTGG**
ACTA1 F	TCTGAATCCCAAAGCCAATC
ACTA1 R	GACTCCATCCCCTGAATCAA
CD36 F	**TGGGATTCCTCATTGCTTTC**
CD36 R	**ACAGCCAACAACACCATGAA**
CPT1B F	AGAACTTGTGCCCGTGATG
CPT1B R	GAAGGGAATCTGCCTCTTTG
ECDH F	**TGAAGACATAGCTTTTGGAGGA**
ECDH R	**CCTATAATGACAGCCCAGTGC**
HPRT1 F	AACAGCGACAAGTCCATTCC
HPRT1 R	TCTTCATCGTCTTGCCTGTG
MCAD F	**CGGAAGGAAGGAGCTTAACA**
MCAD R	**TGCTAATCCAACAGCACCAG**
mFABP F	GACCAAACCCACCACCATTA
mFABP R	GATCTCTGTGTTCTTGAAAGTGC
MYH7 F	**AAGGAAAGATCCTCCGAGC**
MYH7 R	**CGAGTCCACCATCCTCAAG**
MYH15 F	CAAATGGCTTCCTGTTTACAA
MYH15 R	TTTCTCGATTACGCAACATATCA
SERCa2 F	**GCACTCCAAACAAGCCTAGC**
SERCa2 R	**ACAACGCAGCGTATCTTTCC**
SOD2 F	TTGGCAAAAGGGGATGTAAC
SOD2 R	TGGCTCTCCTCCACCATTAG
VLDLR F	**TGGGGATACGGACTGTAAGG**
VLDLR R	**CACAAGAATTTTCCAGGTCCA**

Additional References

27. C. Helmstetter *et al*., Functional changes with feeding in the gastro-intestinal epithelia of the Burmese python (*Python molurus*). *Zoolog. Sci.* **26**, 632 (2009). doi:10.2108/zsj.26.632 Medline

28. B. C. Harrison, M. L. Bell, D. L. Allen, W. C. Byrnes, L. A. Leinwand, Skeletal muscle adaptations in response to voluntary wheel running in myosin heavy chain null mice. *J. Appl. Physiol.* **92**, 313 (2002). Medline

29. L. E. Waspe, C. P. Ordahl, P. C. Simpson, The cardiac beta-myosin heavy chain isogene is induced selectively in alpha 1-adrenergic receptor-stimulated hypertrophy of cultured rat heart myocytes. *J. Clin. Invest.* **85**, 1206 (1990). doi:10.1172/JCI114554 Medline

30. C. M. Harmon, P. Luce, A. H. Beth, N. A. Abumrad, Labeling of adipocyte membranes by sulfo-N-succinimidyl derivatives of long-chain fatty acids: inhibition of fatty acid transport. *J. Membr. Biol.* **121**, 261 (1991). doi:10.1007/BF01951559 Medline

31. L. A. MacMillan-Crow, J. P. Crow, J. D. Kerby, J. S. Beckman, J. A. Thompson, Nitration and inactivation of manganese superoxide dismutase in chronic rejection of human renal allografts. *Proc. Natl. Acad. Sci. U.S.A.* **93**, 11853 (1996). doi:10.1073/pnas.93.21.11853 Medline

32. J. Folch, M. Lees, G. H. Sloane Stanley, A simple method for the isolation and purification of total lipides from animal tissues. *J. Biol. Chem.* **226**, 497 (1957). Medline